

Accurate and Efficient Prediction of Double Excitation Energies Using the Particle-Particle Random Phase Approximation

Jincheng Yu,^{1, a)} Jiachen Li,^{2, a)} Tianyu Zhu,² and Weitao Yang^{1, b)}

¹⁾*Department of Chemistry, Duke University, Durham, North Carolina 27708, United States*

²⁾*Department of Chemistry, Yale University, New Haven, Connecticut 06520, United States*

Double excitations are crucial to understanding numerous chemical, physical, and biological processes, but accurately predicting them remains a challenge. In this work, we explore the particle-particle random phase approximation (ppRPA) as an efficient and accurate approach for computing double excitation energies. We benchmark ppRPA using various exchange-correlation functionals for 21 molecular systems and two point defect systems. Our results show that ppRPA with functionals containing appropriate amounts of exact exchange provides accuracy comparable to high-level wave function methods such as CCSDT and CASPT2, with significantly reduced computational cost. Furthermore, we demonstrate the use of ppRPA starting from an excited ($N - 2$)-electron state calculated by Δ SCF for the first time, as well as its application to double excitations in bulk periodic systems. These findings suggest that ppRPA is a promising tool for the efficient calculation of double and partial double excitation energies in both molecular and bulk systems.

^{a)}These two authors contributed equally

^{b)}Electronic mail: weitao.yang@duke.edu

I. INTRODUCTION

Double excitations, where two electrons are promoted from occupied orbitals to virtual orbitals of the reference state, play a significant role in understanding many important chemical, physical and biological processes, including the photochemistry of conjugated polymers¹⁻⁷, formations of the triplet-pair state in the singlet fission⁸ and conical intersections in coupled electron-nuclear dynamics⁹. Experimentally, directly studying double excitations with spectroscopic methods is challenging, because they are dark and usually cannot be observed in photo-absorption spectroscopy¹⁰. Therefore, the optically forbidden doubly excited states can only be indirectly probed by methods such as photoluminescence¹¹ and spectrally resolved four-wave mixing experiments¹².

The theoretical study of double excitations involves the quasiparticle state named biexciton that is composed of two particles and two holes. The accurate description of biexcitons requires computing four-body correlations¹³, which is a crucial for describing simultaneous propagation of two electrons or two holes. However, the calculation of four-body correlations is a difficult task in the theoretical treatment when many-body effects are important. This leads to significant challenges for single-reference methods to model double excitations. For example, the adiabatic time-dependent density functional theory (TD-DFT)^{14,15}, which considers only singly excited states that consist of one particle and one hole, cannot be applied for the computation of doubly excited states^{16,17}. To address this issue, the spin-flip TD-DFT¹⁸⁻²⁰ that describes double excitations as excitations from high-spin reference states was developed. However, choosing a suitable high-spin reference state is a nontrivial task that has high requirement of chemical intuition²⁰. To go beyond the adiabatic approximation, a dressed TD-DFT method employing frequency-dependent exchange-correlation (XC) kernels has been proposed^{2,4,21,22}. The similar idea of adopting frequency-dependent XC kernels is also used in the Bethe-Salpeter equation (BSE) formalism²³⁻²⁵ to describe doubly excited states^{22,26-28}. In addition to these approaches, the ensemble DFT using weight-dependent local exchange functional^{29,30} and orbital-optimized DFT^{31,32} have also been used to compute double excitation energies.

Approaches based on the wave function theory (WFT) also face challenges when describing doubly excited states. For small systems, highly accurate but computationally expensive methods such as the full configuration interaction (FCI), Monte Carlo CI (MCCI)³³,

semi-stochastic heat-bath CI (SHCI)^{34,35}, iterative CI (iCI)³⁶, can be used to compute excitation energies with high accuracy. Multiconfigurational self-consistent field (MCSCF) methods and their perturbative variants, including the complete-active-space self-consistent field (CASSCF), complete-active-space perturbation theory (CASPT)^{37,38}, and n-electron valence state perturbation theory (NEVPT)^{39–42}, treat all excited states equally, and thus can naturally be used to calculate doubly excited states. However, the computational cost grows exponentially with the number of active electrons and orbitals. Coupled cluster methods (CC)^{43–46} and perturbation theory (PT) methods⁴⁷ are known for their ability to capture the dynamic correlation, and thus are widely employed to calculate excited states. To use these method for describing doubly excited states, one has to go beyond the commonly used second-order approaches so these methods can explicitly account for the two-particle-two-hole configurations. Recently, state-specific CC methods has been demonstrated to predict accurate double excitation energies⁴⁸. With the equation-of-motion (EOM) formalism, the EOM-CC methods^{49–54} provide a systematically improvable approach for predicting single and multi excitations. Although EOM-CCSD includes the two-particle-two-hole configurations in the calculations, the accuracy for double excitations is not sufficient^{55,56}. Therefore, one still needs to use higher-order methods within the EOM-CC scheme^{55–57}, which are computationally demanding.

In addition to the above approaches, the particle-particle random-phase approximation (ppRPA) has the potential to serve as a more computationally efficient pathway to calculate double excitation energies. The ppRPA, which was originally developed to calculate the nuclear many-body correlation energy^{58,59}, has been further developed to describe the electronic correlation energies, and electronic excitation energies in molecular and bulk systems^{60–64}. ppRPA can be equivalently derived from different perspectives such as the two-particle Green’s function⁵⁹ and the EOM ansatz^{58,65}. In the context of DFT, ppRPA can be derived from the adiabatic connection^{60,61} as a counterpart of the commonly used particle-hole random phase approximation (phRPA)^{66,67} and from TD-DFT with the pairing field as the second order derivative of the XC energy with respect to the pairing matrix⁶⁸, which rationalize the practice of using Kohn-Sham orbitals and eigenvalues in ppRPA. The ppRPA correlation energy is exact up to the second order in electron-electron interaction⁶⁰ and is equivalent to the ladder coupled-cluster doubles^{69,70}. For calculations of excitation energies, ppRPA can be considered as an approximation to double-electron-affinity or double-ionization-potential

EOM-CC doubles^{62,71}. In ppRPA, the excitation energies of a given N -electron system can be calculated as the differences between the two-electron addition energies of the $(N - 2)$ -electron system from the particle-particle (pp) channel. Similarly, the excitation energies can also be obtained from the differences between the two-electron removal energies of the $(N + 2)$ -electron system from the hole-hole (hh) channel⁶². The choice of the pp or the hh channels enhances the flexibility of the ppRPA method.

ppRPA has been further developed in many aspects and achieved a lot of success in recent years due to its intrinsic features. By the construction, ppRPA can be understood as a Fock-space embedding method that handles two electrons in a subspace CI manner, seamlessly integrated with DFT for the remaining $(N - 2)$ electrons^{72,73}. As a result, ppRPA offers a highly accurate description of the static correlation for the two non-bonding electrons in diradical systems, and therefore predicts accurate singlet-triplet gaps in diatomic, carbene-like, disjoint and four- π -electron diradicals⁷². In bulk systems, ppRPA has also been shown to accurately describe correlated excited states of point defects^{63,64}. Moreover, since the ppRPA kernel exhibits the correct long-range asymptotic behavior, it can accurately predict charge-transfer (CT) and Rydberg excitation energies^{62,74}. Recently, ppRPA has been employed in the multireference DFT approach, yielding accurate dissociation and excitation energies^{75,76}. The hole-hole channel in ppRPA has also been used to simulate molecular dynamics properties^{77,78}. The formal scaling of ppRPA for computing excitation energies is $\mathcal{O}(N^4)$ with the Davidson algorithm⁷⁹. Development in using active space in ppRPA⁸⁰ and particularly the recent truncation approach⁸¹ has significantly reduced the computational cost without loss of accuracy, making wider applications of the method possible. In the Green’s function theory, ppRPA eigenvalues and eigenvectors have also been utilized to construct the self-energy in the T-matrix approximation to calculate quasiparticle energies^{80,82–84}.

Compared to particle-hole formalisms, one of the major advantages of ppRPA is that it incorporates information from the particle-particle and hole-hole channels, which makes it naturally adept at describing double excitations. It has been shown that ppRPA with traditional XC functionals predicts accurate double excitation energies for small molecules with errors around 0.5 eV^{62,73}, and also for polymer systems⁸⁵. Recently, ppRPA has been further applied to analyze doubly excited states in point defects⁶⁴. In this work, we explore the effectiveness and robustness of ppRPA for providing accurate double excitation energies.

We examine the performance of ppRPA based on a broad range of XC functionals for describing double excitations with a comprehensive benchmark set developed in Refs 13,86, which contains excited states with genuine and partial double excitation characters. In a new direction, we also developed the ppRPA calculations from an excited state calculated within the Δ SCF framework. In particular, in the ppRPA@B3LYP calculation for acrolein, the $(N-2)$ -electron system is obtained by removing two electron from the HOMO-1 orbital of the N -electron system. This is as well justified as ppRPA calculations starting from on a DFT ground state, given the recent theoretical work establishing the foundation of the Δ SCF method⁸⁷. It should open up possibility of describing excited states that are not traditionally accessible.

II. THEORY

Similar to phRPA that is formulated with the density-density response function, ppRPA is formulated with the particle-particle propagator describing the dynamic fluctuation of the pairing matrix $\langle \Psi_0^N | \hat{a}_p \hat{a}_q | \Psi_0^N \rangle$, where Ψ_0^N is the wave function of the N -electron reference state and \hat{a}_p is the annihilation operator in the second-quantization notation. In this paper, we use p, q, r, s for general molecular orbitals, i, j, k, l for occupied orbitals, a, b, c, d for virtual orbitals, and m for the index of the two-electron addition/removal energy. In the frequency space, the time-ordered pairing matrix fluctuation is^{60,61}

$$K_{pqrs}(\omega) = \sum_m \frac{\langle \Psi_0^N | \hat{a}_p \hat{a}_q | \Psi_m^{N+2} \rangle \langle \Psi_m^{N+2} | \hat{a}_s^\dagger \hat{a}_r^\dagger | \Psi_0^N \rangle}{\omega - \Omega_m^{N+2} + i\eta} - \sum_m \frac{\langle \Psi_0^N | \hat{a}_s^\dagger \hat{a}_r^\dagger | \Psi_m^{N-2} \rangle \langle \Psi_m^{N-2} | \hat{a}_p \hat{a}_q | \Psi_0^N \rangle}{\omega - \Omega_m^{N-2} - i\eta} \quad (1)$$

where \hat{a}_p^\dagger is the second quantization creation operator, $\Omega^{N\pm 2}$ is the two-electron addition/removal energy, and η is a positive infinitesimal number.

The pairing matrix fluctuation K of the interacting system can be approximated from the non-interacting K_0 with the Dyson equation^{60,61}

$$K = K^0 + K^0 V K \quad (2)$$

where the interaction $V_{pqrs} = \langle pq|rs \rangle - \langle pq|sr \rangle$ is used and $\langle pq|rs \rangle = \int dx_1 dx_2 \frac{\phi_p^*(x_1) \phi_q^*(x_2) \phi_r(x_1) \phi_s(x_2)}{|r_1 - r_2|}$.

In the direct ppRPA, the exchange term in V in Eq. 2 is neglected⁸⁸.

Eq. 2 can be written as a generalized eigenvalue equation^{60,61}, with a form similar to the

Casida equation in TD-DFT

$$\begin{bmatrix} \mathbf{A} & \mathbf{B} \\ \mathbf{B}^T & \mathbf{C} \end{bmatrix} \begin{bmatrix} \mathbf{X} \\ \mathbf{Y} \end{bmatrix} = \Omega^{N\pm 2} \begin{bmatrix} \mathbf{I} & \mathbf{0} \\ \mathbf{0} & -\mathbf{I} \end{bmatrix} \begin{bmatrix} \mathbf{X} \\ \mathbf{Y} \end{bmatrix} \quad (3)$$

with

$$A_{ab,cd} = \delta_{ac}\delta_{bd}(\epsilon_a + \epsilon_b) + \langle ab||cd \rangle \quad (4)$$

$$B_{ab,kl} = \langle ab||kl \rangle \quad (5)$$

$$C_{ij,kl} = -\delta_{ik}\delta_{jl}(\epsilon_i + \epsilon_j) + \langle ij||kl \rangle \quad (6)$$

where $a < b$, $c < d$, $i < j$, and $k < l$. In the ppRPA calculations, the DFT SCF calculations of the $(N \pm 2)$ -electron states at the ground-state geometry of N -electron system are first performed, then the orbitals and corresponding orbital energies are used in Eq. 3 for calculating two-electron addition energies. The excitation energy is obtained from the difference between the lowest and a higher two-electron addition/removal energy.

For closed-shell $(N - 2)$ -electron systems, Eq. 3 can be expressed in the spin-adapted form⁶⁵. The singlet ppRPA matrix is given by

$$A_{ab,cd}^s = \delta_{ac}\delta_{bd}(\epsilon_a + \epsilon_b) + \frac{1}{\sqrt{(1 + \delta_{ab})(1 + \delta_{cd})}}(\langle ab|cd \rangle + \langle ab|dc \rangle) \quad (7)$$

$$B_{ab,kl}^s = \frac{1}{\sqrt{(1 + \delta_{ab})(1 + \delta_{kl})}}(\langle ab|kl \rangle + \langle ab|lk \rangle) \quad (8)$$

$$C_{ij,kl}^s = -\delta_{ik}\delta_{jl}(\epsilon_i + \epsilon_j) + \frac{1}{\sqrt{(1 + \delta_{ij})(1 + \delta_{kl})}}(\langle ij|kl \rangle + \langle ij|lk \rangle) \quad (9)$$

with $a \leq b$, $c \leq d$, $i \leq j$ and $k \leq l$. The triplet ppRPA matrix is given by

$$A_{ab,cd}^t = \delta_{ac}\delta_{bd}(\epsilon_a + \epsilon_b) + \langle ab||cd \rangle \quad (10)$$

$$B_{ab,kl}^t = \langle ab||kl \rangle \quad (11)$$

$$C_{ij,kl}^t = -\delta_{ik}\delta_{jl}(\epsilon_i + \epsilon_j) + \langle ij||kl \rangle \quad (12)$$

To reduce the computational cost, an active space composed of $N_{\text{occ,act}}$ occupied and $N_{\text{vir,act}}$ virtual orbitals can be employed to construct ppRPA matrices⁸¹. As a result, the indices of the singlet ppRPA matrices in Eq. 7 to Eq. 9 are constrained as

$$a \leq b \leq N_{\text{vir,act}} \text{ and } c \leq d \leq N_{\text{vir,act}} \quad (13)$$

$$i \leq j \leq N_{\text{occ,act}} \text{ and } k \leq l \leq N_{\text{occ,act}} \quad (14)$$

For the triplet ppRPA matrix in Eq. 10 to Eq. 12, the indices are constrained in a similar way. In this work, the active-space ppRPA is used in calculations for point defects. As shown in Ref. 81, the scaling of active-space ppRPA is $\mathcal{O}(N_{\text{act}}^4)$ with the Davidson algorithm, where N_{act} is the number of orbitals in the active space. In addition, two-electron integrals can be efficiently constructed with the resolution of identity or the density-fitting (DF) technique. For the three-index DF matrix, the atomic orbital (AO)-to-molecular orbital (MO) transformation step scales as $\mathcal{O}(N_{\text{aux}}N_{\text{AO}}^2N_{\text{act}})$, where N_{AO} is the number of atomic orbitals and N_{aux} is the number of auxiliary basis functions.

III. COMPUTATIONAL DETAILS

For double excitation energies of molecular systems, the geometries are from Ref. 13. The SCF calculations of the $(N-2)$ -electron systems were performed with the aug-cc-pVTZ basis set^{89,90} using the PySCF package^{91,92}. All the calculations were performed in the full space with the Davidson algorithm⁷⁹. Results from aug-cc-pVQZ calculations are documented in the supporting information (SI). Geometries of point defects were taken from Ref.⁶⁴. For the nitrogen-vacancy (NV^-) in diamond, the $(N+2)$ -electron ground state was used and excitation energies were calculated within the hole-hole channel in ppRPA. For the carbon vacancy (VC) in diamond, the geometry with D_{2d} symmetry was used, and the $(N-2)$ -electron ground state was used and excitation energies were calculated within the particle-particle channel in ppRPA. All periodic defect calculations were performed with Γ -point sampling and Gaussian density fitting, with cc-pVDZ basis set⁹³ and the corresponding cc-pVDZ-RI auxiliary basis set⁹⁴. In this work, all ground-state DFT calculations were carried out using the PySCF quantum chemistry software package^{91,92}.

IV. RESULTS

A. Double excitation of molecular systems

Double excitation energies of 21 molecules from Ref. 13 were calculated with ppRPA. Eight functionals, including three hybrid functionals, one generalized gradient approximation (GGA), one meta-GGA, and three range-separated hybrid functionals, were used to perform SCF calculations on the $(N-2)$ -electron systems as starting points of ppRPA calculations.

Excitation energies, mean signed errors (MSEs), and mean absolute errors (MAEs) from these calculations are tabulated in Table I.

Two types of double excitations are investigated in this study: genuine double excitations (gd), which are primarily characterized by doubly excited configurations, and partial double excitations (pd), which exhibit significant contributions from singly excited configurations. This classification is based on CC3 calculations¹³. ppRPA provides comparable accuracy in describing both types of double excitations. This capability arises from ppRPA’s strength in calculating states with multi-reference character. Within ppRPA, two electrons are treated accurately in a CI framework, while the remaining $N - 2$ electrons are described using DFT.

Among the eight functionals we tested, TPSSh produces the lowest MAE (0.350 eV) and ω B97X-D produces the highest MAE (0.530 eV), indicating a small starting point dependence in ppRPA for predicting double excitation energies. The difference between the two values is only 0.180 eV, much smaller than the functional differences between DFT-based approaches reported in Refs 30–32. One of the reasons for the different accuracy of different functionals may be the percentage of the exact exchange. In Table II, we list the percentages of the exact exchange of the functionals studied. For ppRPA@PBE and ppRPA@SCAN, where the functionals have no exact exchange, the MAEs are both around 0.40 eV. The difference is that ppRPA@PBE underestimates the double excitation energies, while ppRPA@SCAN overestimates them. For ppRPA calculations starting from SCF results obtained from hybrid functionals, ppRPA@M06-2X where the functional contains 54% exact exchange produces the largest MAE and MSE. With the functionals containing 20% and 10% exact exchange respectively, ppRPA@B3LYP and ppRPA@TPSSh provides similar accuracy. The MAEs differ by around 0.01 eV, and the MSEs differ by less than 0.1 eV. Among the three range-separated hybrid functionals, two of them, namely CAM-B3LYP and ω B97X-D, have significant amount (65% and 100%) of exact exchange in the long range. Both the MAEs from ppRPA@CAM-B3LYP and ppRPA@ ω B97X-D are over 0.5 eV, which is similar to that from ppRPA@M06-2X. For ppRPA@HSE03, where the functional does not contain the exact exchange in the long range, the MAE is similar to those from ppRPA@B3LYP and ppRPA@TPSSh. To conclude, ppRPA starting from hybrid functionals with around 10%~20% exact exchange can provide more accurate double excitation energies compared to GGAs and meta-GGAs, while increasing the amount of exact exchange may cause the accuracy to decrease. This agrees with previous results of ppRPA for predicting double

excitation energies of small molecules⁶². For range-separated functionals, a high fraction of exact exchange in the long range can lead to less accurate descriptions of double excitation energies.

Here we compare the results from ppRPA with those from other methods. In Ref. 13, Kossoski et al. provide reference energies for double excitations from 11 WFT methods. Comparing the MAEs from ppRPA and the 11 WFT methods, we find that ppRPA starting from DFAs with proper amount of exact exchange is more accurate than state-averaged CASSCF (SA-CASSCF) and CC3, whose MAEs are 0.48 eV and 0.56 eV respectively. With carefully selected DFAs, ppRPA provides similar accuracy as CCSDT and CASPT2 for double excitation energies. Because of the computationally favorable cost, ppRPA can be an efficient alternative to WFT methods for predicting double excitations.

In all the calculations performed in this work, the $^1A'$ ($\pi \rightarrow \pi^*$) state of acrolein from ppRPA@B3LYP is a special one. As shown in Fig. 1, after taking two electrons away, orbital misalignment happens in the $(N - 2)$ -electron system. From the SCF calculation on the N -electron system, one can know that the π orbital from which the electrons are excited from is the highest occupied molecular orbital (HOMO). Based on this, one would intuitively take two electrons away from the HOMO to form the $(N - 2)$ -electron system. However, in the $(N - 2)$ -electron system, the orders of the π orbital and the orbital below it are switched. Therefore, we used the Δ SCF approach using the maximum overlap method (MOM)⁹⁵ implemented in PySCF to obtain the proper starting-point configuration from Δ SCF⁸⁷, which is as a doubly excited state of the $(N - 2)$ -electron system. The ppRPA equations for such calculations based on Δ SCF approach remain the same as in Eqs. (3-12).

TABLE I: Vertical double excitation energies calculated with ppRPA using the aug-cc-pVTZ basis set. TBE stands for theoretical best estimate. MAE and MSE stand for mean absolute error and mean signed error. pd and gd stand for partial double excitation and genuine double excitation¹³. MAEs and MSEs are calculated with respect to TBEs. Some results are not available (denoted as N/A) due to the convergence issue of the $(N - 2)$ -electron systems. All values are in eV.

system	state	type	functional								
			TBE	B3LYP	M06-2X	TPSSh	PBE	SCAN	CAM-B3LYP	HSE03	ω B97X-D
acrolein	$^1A'$	pd	7.928	7.945	N/A	N/A	N/A	N/A	8.159	N/A	8.183

TABLE I continued:

system	state	type	TBE	B3LYP	M06-2X	TPSSh	PBE	SCAN	CAM-B3LYP	HSE03	ω B97X-D
benzoquinone	1A_g	gd	4.566	5.976	6.753	5.565	4.904	5.461	N/A	6.098	N/A
borole	1A_1	pd	6.484	7.395	7.388	7.481	N/A	7.640	7.469	7.566	7.520
	1A_1	gd	4.708	4.656	4.809	4.702	N/A	4.757	4.787	4.765	4.858
butadiene	1A_g	pd	6.515	6.484	6.612	6.506	6.162	6.595	6.701	6.630	6.748
cyclobutadiene	1A_g	gd	4.036	4.018	4.068	4.084	3.923	4.158	4.058	4.096	4.114
cyclopentadiene	1A_1	pd	6.451	6.489	6.653	6.534	6.238	6.663	6.652	6.627	6.673
cyclopentadienethione	1A_1	pd	5.329	N/A	4.269	N/A	N/A	N/A	4.310	N/A	4.206
cyclopentadienone	1A_1	pd	6.714	7.691	7.686	N/A	N/A	N/A	7.762	N/A	7.809
	1A_1	gd	5.009	5.363	5.533	N/A	N/A	N/A	5.488	N/A	5.439
diazete	1A_1	gd	6.605	6.733	N/A	N/A	N/A	N/A	6.755	6.872	6.886
ethylene	1A_g	gd	12.899	12.737	12.204	12.985	12.968	13.491	12.494	12.880	12.641
formaldehyde	1A_1	gd	10.426	10.371	10.089	10.672	10.398	10.832	10.245	10.498	10.479
glyoxal	1A_g	gd	5.492	5.810	6.329	5.584	4.982	5.628	6.374	5.947	6.247
hexatriene	1A_g	pd	5.435	5.046	5.581	4.964	4.546	4.921	5.560	5.169	5.603
naphthalene	1A_g	pd	6.748	6.414	7.067	6.326	7.408	6.283	7.000	6.573	6.997
nitrosomethan	$^1A'$	gd	4.732	4.247	4.147	4.296	4.412	4.455	4.202	4.299	4.239
nitrous acid	$^1A'$	gd	7.969	8.528	8.647	8.572	8.247	8.690	8.627	8.629	8.666
nitroxyl	$^1A'$	gd	4.333	4.638	4.624	4.708	4.575	4.757	4.639	4.699	4.732
octatetraene	1A_g	pd	4.68	4.140	4.770	4.013	3.594	3.907	4.744	4.235	4.809
oxalyl fluoride	1A_1	gd	8.923	9.556	9.299	9.373	8.937	9.619	9.500	9.786	9.771
pyrazine	1A_g	pd	8.48	8.679	9.000	N/A	N/A	N/A	9.060	8.741	9.025
	1A_g	gd	7.904	8.607	N/A	8.430	N/A	N/A	8.921	N/A	8.914
tetrazine	1A_g	gd	4.951	5.216	5.751	4.984	4.467	4.875	5.693	5.333	5.621
	1B_3	gd	6.215	7.004	7.530	6.791	6.152	6.756	7.514	7.155	7.429
	3B_3	gd	5.848	5.989	6.577	5.753	5.083	5.702	6.536	6.145	6.437
MSE				0.227	0.367	0.150	-0.190	0.199	0.342	0.297	0.374
MAE				0.393	0.600	0.361	0.378	0.436	0.520	0.425	0.530

TABLE II. Percentages of the exact exchange in various functionals.

functional	exact exchange%
B3LYP	20%
M06-2X	54%
TPSSh	10%
PBE	0%
SCAN	0%
CAM-B3LYP	short range 19%, long range 65%
HSE03	short range 25%, long range 0%
ω B97X-D	short range 22.2%, long range 100%

We further visualize double excitations obtained from ppRPA using natural transition orbitals (NTOs) developed in Ref. 64. NTOs of double excitations for the 1A_g state in ethylene and the 1A_g state in hexatriene are shown in Fig. 2. For the 1A_g state in ethylene, NTOs corresponding to (π^*, π^*) has a NTO weight of 0.72, which agrees with its genuine double excitation nature. For the partial double excited 1A_g state in hexatriene, NTOs corresponding to (π^*, π^*) provides a smaller NTO weight of 0.39.

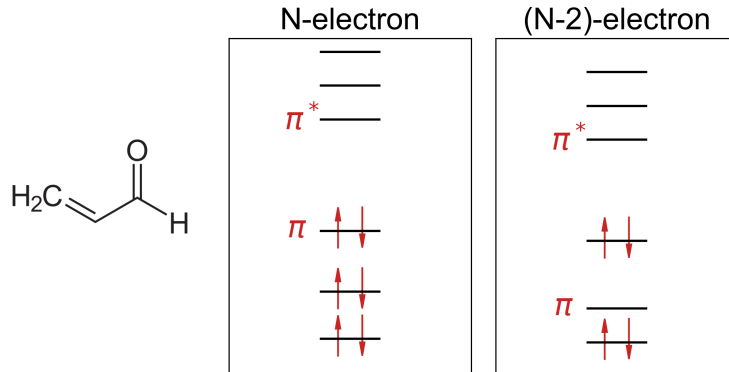


FIG. 1. Valence energy levels in N -electron and $(N - 2)$ -electron systems of acrolein obtained from B3LYP (energy levels are qualitative only). In the $(N - 2)$ -electron system, two electrons are removed from the π orbital.

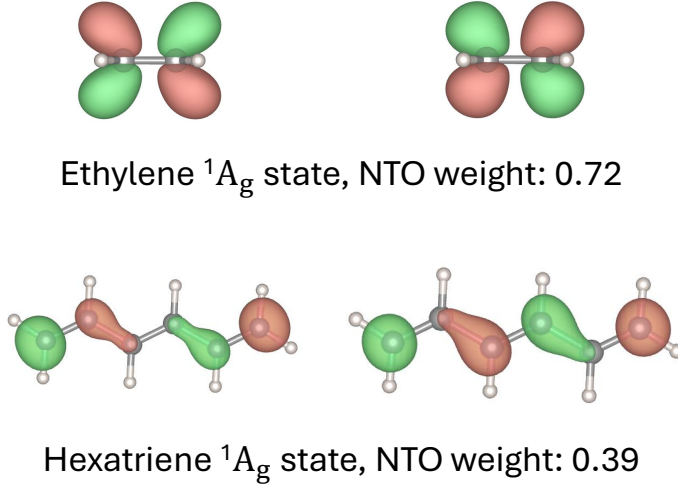


FIG. 2. Natural transition orbitals of double excitations for the 1A_g state in ethylene and the 1A_g state in hexatriene obtained from ppRPA@M06-2X. The aug-cc-pVTZ basis set was used. Isosurface value is 0.06 a.u.

B. Double excitations in point defects

We further examine the performance of ppRPA for describing double excitations in periodic bulk systems. Two point defect systems are tested: NV^- in diamond and VC in diamond with D_{2d} symmetry, whose defect energy levels are shown in Fig. 3. Vertical double excitation energies of defect states involving with double excitation characters obtained from ppRPA based on different functionals compared with experiment values are tabulated in Table III. To correct the finite supercell-size error, a linear fitting two-point supercell-size extrapolation scheme $E(1/N_{\text{atom}}) = E_{\infty} + a/N_{\text{atom}}$ was employed, which has been utilized to compute excitation energies of defect systems in the thermodynamic limit^{63,64,99,100}. For the NV^- in diamond, the hole-hole channel in ppRPA is used to calculate excitation energies. The 1A_1 state in the NV^- in diamond is shown to have a strong multireference character^{64,101}. As shown in Table III, ppRPA based on different functionals provides similar descriptions for the 1A_1 state, showing that the contribution of the doubly-excited configuration $|e_x\bar{e}_xe_y\bar{e}_y\rangle$ is around 15%. Excitation energies obtained from ppRPA with different functionals are around 1.8 to 2.1 eV, which shows a much smaller starting point dependence than TD-DFT^{64,99}. For the VC in diamond, as shown in Ref. 64, the ground state 1A_1 has a strong double excitation energy. Single-reference methods fail to capture doubly-excited configurations $|e_x\bar{e}_x\rangle$

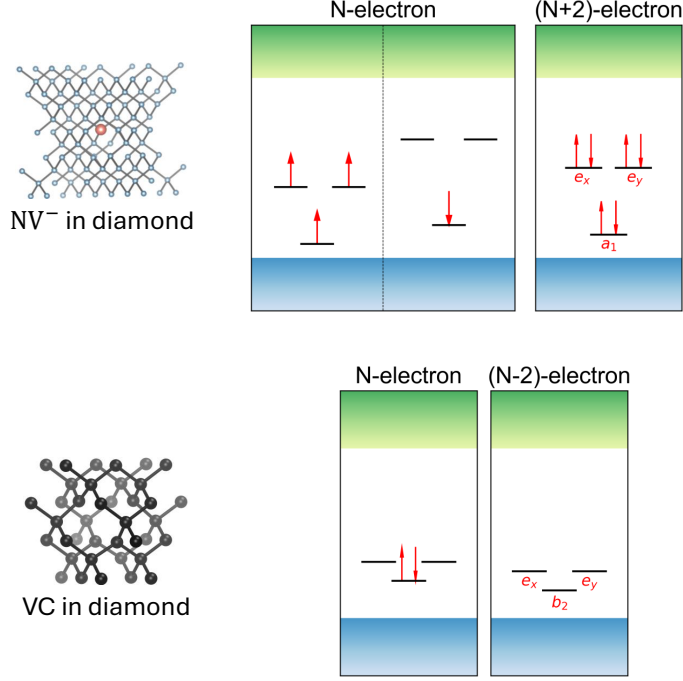


FIG. 3. Illustration of defect energy levels and ground-state electron configurations of NV^- and VC in diamond (energy levels are qualitative only).

and $|e_y\bar{e}_y\rangle$, which is the main source of large errors in TD-DFT⁶⁴. ppRPA based on different functionals shows that the $^1\text{A}_1$ state has 85% contributions from the $|b_2\bar{b}_2\rangle$ configuration as well as 15% contributions from doubly-excited configurations $|e_x\bar{e}_x\rangle$ and $|e_y\bar{e}_y\rangle$. With a proper description for the ground state, ppRPA based on local and non-local functionals provides errors around 0.5 eV and 0.1 eV for the excitation energy of the ^1E state, which are much smaller than the 1 eV error in TD-DFT⁶⁴. For defect systems, ppRPA based on B3LYP and HSE03 provide smallest errors for excitation energies involving with double excitation characters, agreeing well with the results for molecular systems in Section IV A.

TABLE III. Vertical excitation energies and dominant configuration contributions of defect states involving with double excitation characters in NV^- and VC in diamond obtained from the ppRPA approach based on different functionals. The geometry with D_{2d} symmetry was employed for VC in diamond. The cc-pVDZ basis set was used. All values of excitation energies are in eV.

NV^- in diamond	$^1\text{A}_1$ excitation	dominant configuration in $^1\text{A}_1$		
		$ a_1\bar{a}_1e_x\bar{e}_x\rangle$	$ a_1\bar{a}_1e_y\bar{e}_y\rangle$	$ e_x\bar{e}_xe_y\bar{e}_y\rangle$
experiment ^{96,97}	1.76~1.85			
PBE	1.67	33.4%	33.4%	11.0%
B3LYP	1.97	34.6%	34.6%	13.4%
CAM-B3LYP	2.09	33.8%	33.8%	16.5%
HSE03	1.96	34.9%	34.8%	12.0%
M06	2.08	33.5%	33.5%	15.0%
M06-2X	1.93	31.8%	31.8%	13.9%
SCAN	1.77	36.1%	36.0%	8.7%
TPSSh	1.83	35.0%	34.9%	10.1%
$\omega\text{B97X-D}$	2.05	33.5%	33.5%	11.9%
VC in diamond	^1E excitation	dominant configuration in $^1\text{A}_1$		
		$ b_2\bar{b}_2\rangle$	$ e_x\bar{e}_x\rangle$	$ e_y\bar{e}_y\rangle$
experiment ⁹⁸	2.20			
PBE	1.75	90.0%	6.0%	6.0%
B3LYP	2.12	85.3%	7.5%	7.5%
CAM-B3LYP	2.35	83.3%	8.5%	8.5%
HSE03	2.09	85.4%	7.5%	7.5%
M06	2.16	83.3%	8.4%	8.4%
M06-2X	2.31	83.1%	8.4%	8.4%
SCAN	1.82	90.0%	5.7%	5.7%
TPSSh	1.87	88.2%	6.4%	6.4%
$\omega\text{B97X-D}$	2.33	82.9%	8.4%	8.4%

V. CONCLUSIONS

In this study, we demonstrated ppRPA as an accurate and computationally efficient method for calculating double excitation energies in molecular and bulk systems. Our benchmark of 21 molecular systems using different DFAs revealed that ppRPA with functionals containing 10-20% exact exchange offers the best accuracy for molecular systems. Errors of ppRPA based on B3LYP, TPSSH and HSE03 are only around 0.40 eV, comparable to computationally demanding WFT methods. In particular, in the calculation of ppRPA@B3LYP for acrolein, the doubly excited state was obtained from ppRPA starting with a non-ground state determinant, which opens up new possibilities for calculating excitation energies. Additionally, ppRPA was shown to be effective in describing correlated states with double excitation characters in point defects on the equal footing. This work establishes ppRPA as an accurate and low-cost tool for investigating double excitations of both molecular and periodic systems.

SUPPORTING INFORMATION

See the Supporting Information for excitation energies of point defect systems and double excitation energies of molecular systems using aug-cc-pVQZ basis set obtained from ppRPA.

ACKNOWLEDGMENTS

J.Y. and W.Y. acknowledge the support from the National Science Foundation (Grant No. CHE-2154831). T.Z. and J.L. are supported by the National Science Foundation (Grant No. CHE-2337991) and a start-up fund from Yale University. J.L. also acknowledges support from the Tony Massini Postdoctoral Fellowship in Data Science.

DATA AVAILABILITY STATEMENT

The data that support the findings of this study are available from the corresponding author upon reasonable request.

REFERENCES

- ¹R. J. Cave and E. R. Davidson, “Theoretical investigation of several low-lying states of trans, trans-1, 3,5-hexatriene,” *J. Phys. Chem.* **92**, 614–620 (1988).
- ²R. J. Cave, F. Zhang, N. T. Maitra, and K. Burke, “A dressed TDDFT treatment of the 21Ag states of butadiene and hexatriene,” *Chem. Phys. Lett.* **389**, 39–42 (2004).
- ³J. Lappe and R. J. Cave, “On the Vertical and Adiabatic Excitation Energies of the 2Ag State of trans-1,3-Butadiene,” *J. Phys. Chem. A* **104**, 2294–2300 (2000).
- ⁴N. T. Maitra, F. Zhang, R. J. Cave, and K. Burke, “Double excitations within time-dependent density functional theory linear response,” *J. Chem. Phys.* **120**, 5932–5937 (2004).
- ⁵J. H. Starcke, M. Wormit, J. Schirmer, and A. Dreuw, “How much double excitation character do the lowest excited states of linear polyenes have?” *Chem. Phys. Electron Correlation and Multimode Dynamics in Molecules*, **329**, 39–49 (2006).
- ⁶G. Mazur, M. Makowski, R. Włodarczyk, and Y. Aoki, “Dressed TDDFT study of low-lying electronic excited states in selected linear polyenes and diphenylopolynes,” *Int. J. Quantum Chem.* **111**, 819–825 (2011).
- ⁷C. Angeli, “An analysis of the dynamic σ polarization in the V state of ethene,” *Int. J. Quantum Chem.* **110**, 2436–2447 (2010).
- ⁸M. B. Smith and J. Michl, “Singlet Fission,” *Chem. Rev.* **110**, 6891–6936 (2010).
- ⁹B. G. Levine, C. Ko, J. Quenneville, and T. J. Martínez, “Conical intersections and double excitations in time-dependent density functional theory,” *Mol. Phys.* **104**, 1039–1051 (2006).
- ¹⁰P.-F. Loos and X. Blase, “Dynamical correction to the Bethe–Salpeter equation beyond the plasmon-pole approximation,” *J. Chem. Phys.* **153**, 114120 (2020).
- ¹¹R. C. Miller, D. A. Kleinman, A. C. Gossard, and O. Munteanu, “Biexcitons in GaAs quantum wells,” *Phys. Rev. B* **25**, 6545–6547 (1982).
- ¹²B. F. Feuerbacher, J. Kuhl, and K. Ploog, “Biexcitonic contribution to the degenerate-four-wave-mixing signal from a GaAs/Al_xGa_{1-x}As quantum well,” *Phys. Rev. B* **43**, 2439–2441 (1991).
- ¹³F. Kossoski, M. Boggio-Pasqua, P.-F. Loos, and D. Jacquemin, “Reference Energies for Double Excitations: Improvement and Extension,” *J. Chem. Theory Comput.* **20**, 5655–

5678 (2024).

- ¹⁴M. E. Casida, “Time-dependent density functional response theory for molecules,” in *Recent Advances In Density Functional Methods: (Part I)* (World Scientific, 1995) pp. 155–192.
- ¹⁵C. A. Ullrich, *Time-Dependent Density-Functional Theory: Concepts and Applications* (OUP Oxford, 2011).
- ¹⁶E. Runge and E. K. U. Gross, “Density-Functional Theory for Time-Dependent Systems,” *Phys. Rev. Lett.* **52**, 997–1000 (1984).
- ¹⁷M. Petersilka, U. J. Gossmann, and E. K. U. Gross, “Excitation Energies from Time-Dependent Density-Functional Theory,” *Phys. Rev. Lett.* **76**, 1212–1215 (1996).
- ¹⁸F. Wang and T. Ziegler, “Time-dependent density functional theory based on a non-collinear formulation of the exchange-correlation potential,” *J. Chem. Phys.* **121**, 12191–12196 (2004).
- ¹⁹N. Minezawa and M. S. Gordon, “Optimizing Conical Intersections by Spin-Flip Density Functional Theory: Application to Ethylene,” *J. Phys. Chem. A* **113**, 12749–12753 (2009).
- ²⁰M. Huix-Rotllant, B. Natarajan, A. Ipatov, C. M. Wawire, T. Deutsch, and M. E. Casida, “Assessment of noncollinear spin-flip Tamm–Dancoff approximation time-dependent density-functional theory for the photochemical ring-opening of oxirane,” *Phys. Chem. Chem. Phys.* **12**, 12811–12825 (2010).
- ²¹P. Romaniello, D. Sangalli, J. A. Berger, F. Sottile, L. G. Molinari, L. Reining, and G. Onida, “Double excitations in finite systems,” *J. Chem. Phys.* **130**, 044108 (2009).
- ²²D. Sangalli, P. Romaniello, G. Onida, and A. Marini, “Double excitations in correlated systems: A many-body approach,” *J. Chem. Phys.* **134**, 034115 (2011).
- ²³E. E. Salpeter and H. A. Bethe, “A Relativistic Equation for Bound-State Problems,” *Phys. Rev.* **84**, 1232–1242 (1951).
- ²⁴X. Blase, I. Duchemin, and D. Jacquemin, “The Bethe–Salpeter equation in chemistry: Relations with TD-DFT, applications and challenges,” *Chem. Soc. Rev.* **47**, 1022–1043 (2018).
- ²⁵X. Blase, I. Duchemin, D. Jacquemin, and P.-F. Loos, “The Bethe–Salpeter Equation Formalism: From Physics to Chemistry,” *J. Phys. Chem. Lett.* **11**, 7371–7382 (2020).
- ²⁶D. Zhang, S. N. Steinmann, and W. Yang, “Dynamical second-order Bethe–Salpeter equation kernel: A method for electronic excitation beyond the adiabatic approximation,” *J.*

- Chem. Phys. **139**, 154109 (2013).
- ²⁷J. Authier and P.-F. Loos, “Dynamical kernels for optical excitations,” J. Chem. Phys. **153**, 184105 (2020).
- ²⁸S. J. Bintrim and T. C. Berkelbach, “Full-frequency dynamical Bethe–Salpeter equation without frequency and a study of double excitations,” J. Chem. Phys. **156**, 044114 (2022).
- ²⁹F. Sagredo and K. Burke, “Accurate double excitations from ensemble density functional calculations,” J. Chem. Phys. **149** (2018).
- ³⁰C. Marut, B. Senjean, E. Fromager, and P.-F. Loos, “Weight dependence of local exchange–correlation functionals in ensemble density-functional theory: double excitations in two-electron systems,” Faraday Discuss. **224**, 402–423 (2020).
- ³¹J. Zhang, Z. Tang, X. Zhang, H. Zhu, R. Zhao, Y. Lu, and J. Gao, “Target state optimized density functional theory for electronic excited and diabatic states,” J. Chem. Theory Comput. **19**, 1777–1789 (2023).
- ³²D. Hait and M. Head-Gordon, “Excited State Orbital Optimization via Minimizing the Square of the Gradient: General Approach and Application to Singly and Doubly Excited States via Density Functional Theory,” J. Chem. Theory Comput. **16**, 1699–1710 (2020).
- ³³J. P. Coe, A. Moreno Carrascosa, M. Simmermacher, A. Kirrander, and M. J. Paterson, “Efficient Computation of Two-Electron Reduced Density Matrices via Selected Configuration Interaction,” J. Chem. Theory Comput. **18**, 6690–6699 (2022).
- ³⁴A. A. Holmes, C. J. Umrigar, and S. Sharma, “Excited states using semistochastic heat-bath configuration interaction,” J. Chem. Phys. **147**, 164111 (2017).
- ³⁵A. D. Chien, A. A. Holmes, M. Otten, C. J. Umrigar, S. Sharma, and P. M. Zimmerman, “Excited States of Methylene, Polyenes, and Ozone from Heat-Bath Configuration Interaction,” J. Phys. Chem. A **122**, 2714–2722 (2018).
- ³⁶N. Zhang, W. Liu, and M. R. Hoffmann, “Iterative Configuration Interaction with Selection,” J. Chem. Theory Comput. **16**, 2296–2316 (2020).
- ³⁷Kerstin. Andersson, P. A. Malmqvist, B. O. Roos, A. J. Sadlej, and Krzysztof. Wolinski, “Second-order perturbation theory with a CASSCF reference function,” J. Phys. Chem. **94**, 5483–5488 (1990).
- ³⁸K. Andersson, P.-Å. Malmqvist, and B. O. Roos, “Second-order perturbation theory with a complete active space self-consistent field reference function,” J. Chem. Phys. **96**, 1218–1226 (1992).

- ³⁹C. Angeli, R. Cimiraglia, S. Evangelisti, T. Leininger, and J.-P. Malrieu, "Introduction of n-electron valence states for multireference perturbation theory," *J. Chem. Phys.* **114**, 10252–10264 (2001).
- ⁴⁰C. Angeli, R. Cimiraglia, and J.-P. Malrieu, "*N*-electron valence state perturbation theory: A fast implementation of the strongly contracted variant," *Chem. Phys. Lett.* **350**, 297–305 (2001).
- ⁴¹C. Angeli, R. Cimiraglia, and J.-P. Malrieu, "N-electron valence state perturbation theory: A spinless formulation and an efficient implementation of the strongly contracted and of the partially contracted variants," *J. Chem. Phys.* **117**, 9138–9153 (2002).
- ⁴²C. Angeli, B. Bories, A. Cavallini, and R. Cimiraglia, "Third-order multireference perturbation theory: The n-electron valence state perturbation-theory approach," *J. Chem. Phys.* **124**, 054108 (2006).
- ⁴³J. Čížek, "On the Correlation Problem in Atomic and Molecular Systems. Calculation of Wavefunction Components in Ursell-Type Expansion Using Quantum-Field Theoretical Methods," *J. Chem. Phys.* **45**, 4256–4266 (1966).
- ⁴⁴R. J. Bartlett and M. Musiał, "Coupled-cluster theory in quantum chemistry," *Rev. Mod. Phys.* **79**, 291–352 (2007).
- ⁴⁵P.-F. Loos, A. Scemama, A. Blondel, Y. Garniron, M. Caffarel, and D. Jacquemin, "A Mountaineering Strategy to Excited States: Highly Accurate Reference Energies and Benchmarks," *J. Chem. Theory Comput.* **14**, 4360–4379 (2018).
- ⁴⁶P.-F. Loos, F. Lipparini, M. Boggio-Pasqua, A. Scemama, and D. Jacquemin, "A Mountaineering Strategy to Excited States: Highly Accurate Energies and Benchmarks for Medium Sized Molecules," *J. Chem. Theory Comput.* **16**, 1711–1741 (2020).
- ⁴⁷I. Shavitt and R. J. Bartlett, *Many-body methods in chemistry and physics: MBPT and coupled-cluster theory* (Cambridge university press, 2009).
- ⁴⁸Y. Damour, A. Scemama, D. Jacquemin, F. Kossoski, and P.-F. Loos, "State-Specific Coupled-Cluster Methods for Excited States," *J. Chem. Theory Comput.* **20**, 4129–4145 (2024).
- ⁴⁹O. Christiansen, H. Koch, and P. Jørgensen, "The second-order approximate coupled cluster singles and doubles model CC2," *Chem. Phys. Lett.* **243**, 409–418 (1995).
- ⁵⁰C. Hättig and F. Weigend, "CC2 excitation energy calculations on large molecules using the resolution of the identity approximation," *J. Chem. Phys.* **113**, 5154–5161 (2000).

- ⁵¹G. D. Purvis, III and R. J. Bartlett, “A full coupled-cluster singles and doubles model: The inclusion of disconnected triples,” J. Chem. Phys. **76**, 1910–1918 (1982).
- ⁵²G. E. Scuseria, A. C. Scheiner, T. J. Lee, J. E. Rice, and H. F. Schaefer, III, “The closed-shell coupled cluster single and double excitation (CCSD) model for the description of electron correlation. A comparison with configuration interaction (CISD) results,” J. Chem. Phys. **86**, 2881–2890 (1987).
- ⁵³H. Koch and P. Jørgensen, “Coupled cluster response functions,” J. Chem. Phys. **93**, 3333–3344 (1990).
- ⁵⁴J. F. Stanton and R. J. Bartlett, “The equation of motion coupled-cluster method. A systematic biorthogonal approach to molecular excitation energies, transition probabilities, and excited state properties,” J. Chem. Phys. **98**, 7029–7039 (1993).
- ⁵⁵P.-F. Loos, D. A. Matthews, F. Lipparini, and D. Jacquemin, “How accurate are eom-cc4 vertical excitation energies?” J. Chem. Phys. **154** (2021).
- ⁵⁶P.-F. Loos, F. Lipparini, D. A. Matthews, A. Blondel, and D. Jacquemin, “A mountaineering strategy to excited states: Revising reference values with eom-cc4,” J. Chem. Theory Comput. **18**, 4418–4427 (2022).
- ⁵⁷V. Rishi, A. Perera, M. Nooijen, and R. J. Bartlett, “Excited states from modified coupled cluster methods: Are they any better than eom ccSD?” J. Chem. Phys. **146** (2017).
- ⁵⁸P. Ring and P. Schuck, *The nuclear many-body problem* (Springer Science & Business Media, 2004).
- ⁵⁹S. R. P. G. Ripka, J.-P. Blaizot, and G. Ripka, *Quantum Theory of Finite Systems* (MIT Press, 1986).
- ⁶⁰H. van Aggelen, Y. Yang, and W. Yang, “Exchange-correlation energy from pairing matrix fluctuation and the particle-particle random-phase approximation,” Phys. Rev. A **88**, 030501 (2013).
- ⁶¹H. van Aggelen, Y. Yang, and W. Yang, “Exchange-correlation energy from pairing matrix fluctuation and the particle-particle random phase approximation,” J. Chem. Phys. **140**, 18A511 (2014).
- ⁶²Y. Yang, H. van Aggelen, and W. Yang, “Double, Rydberg and charge transfer excitations from pairing matrix fluctuation and particle-particle random phase approximation,” J. Chem. Phys. **139**, 224105 (2013).

- ⁶³J. Li, Y. Jin, J. Yu, W. Yang, and T. Zhu, “Accurate Excitation Energies of Point Defects from Fast Particle–Particle Random Phase Approximation Calculations,” *J. Phys. Chem. Lett.* **15**, 2757–2764 (2024).
- ⁶⁴J. Li, Y. Jin, J. Yu, W. Yang, and T. Zhu, “Particle–Particle Random Phase Approximation for Predicting Correlated Excited States of Point Defects,” *J. Chem. Theory Comput.* (2024), 10.1021/acs.jctc.4c00829.
- ⁶⁵Y. Yang, H. van Aggelen, S. N. Steinmann, D. Peng, and W. Yang, “Benchmark tests and spin adaptation for the particle-particle random phase approximation,” *J. Chem. Phys.* **139**, 174110 (2013).
- ⁶⁶D. Bohm and D. Pines, “A Collective Description of Electron Interactions. I. Magnetic Interactions,” *Phys. Rev.* **82**, 625–634 (1951).
- ⁶⁷X. Ren, P. Rinke, C. Joas, and M. Scheffler, “Random-phase approximation and its applications in computational chemistry and materials science,” *J. Mater. Sci.* **47**, 7447–7471 (2012).
- ⁶⁸D. Peng, H. van Aggelen, Y. Yang, and W. Yang, “Linear-response time-dependent density-functional theory with pairing fields,” *J. Chem. Phys.* **140**, 18A522 (2014).
- ⁶⁹D. Peng, S. N. Steinmann, H. van Aggelen, and W. Yang, “Equivalence of particle-particle random phase approximation correlation energy and ladder-coupled-cluster doubles,” *J. Chem. Phys.* **139**, 104112 (2013).
- ⁷⁰G. E. Scuseria, T. M. Henderson, and I. W. Bulik, “Particle-particle and quasiparticle random phase approximations: Connections to coupled cluster theory,” *J. Chem. Phys.* **139**, 104113 (2013).
- ⁷¹T. C. Berkelbach, “Communication: Random-phase approximation excitation energies from approximate equation-of-motion coupled-cluster doubles,” *J. Chem. Phys.* **149**, 041103 (2018).
- ⁷²Y. Yang, D. Peng, E. R. Davidson, and W. Yang, “Singlet–Triplet Energy Gaps for Diradicals from Particle–Particle Random Phase Approximation,” *J. Phys. Chem. A* **119**, 4923–4932 (2015).
- ⁷³D. Zhang and W. Yang, “Accurate and efficient calculation of excitation energies with the active-space particle-particle random phase approximation,” *J. Chem. Phys.* **145**, 144105 (2016).

- ⁷⁴Y. Yang, A. Dominguez, D. Zhang, V. Lutsker, T. A. Niehaus, T. Frauenheim, and W. Yang, “Charge transfer excitations from particle-particle random phase approximation—Opportunities and challenges arising from two-electron deficient systems,” *J. Chem. Phys.* **146**, 124104 (2017).
- ⁷⁵Z. Chen, D. Zhang, Y. Jin, Y. Yang, N. Q. Su, and W. Yang, “Multireference Density Functional Theory with Generalized Auxiliary Systems for Ground and Excited States,” *J. Phys. Chem. Lett.* **8**, 4479–4485 (2017).
- ⁷⁶J. Li, Z. Chen, and W. Yang, “Multireference Density Functional Theory for Describing Ground and Excited States with Renormalized Singles,” *J. Phys. Chem. Lett.* **13**, 894–903 (2022).
- ⁷⁷J. K. Yu, C. Bannwarth, E. G. Hohenstein, and T. J. Martínez, “Ab Initio Nonadiabatic Molecular Dynamics with Hole–Hole Tamm–Dancoff Approximated Density Functional Theory,” *J. Chem. Theory Comput.* **16**, 5499–5511 (2020).
- ⁷⁸C. Bannwarth, J. K. Yu, E. G. Hohenstein, and T. J. Martínez, “Hole–hole Tamm–Dancoff-approximated density functional theory: A highly efficient electronic structure method incorporating dynamic and static correlation,” *J. Chem. Phys.* **153**, 024110 (2020).
- ⁷⁹Y. Yang, D. Peng, J. Lu, and W. Yang, “Excitation energies from particle-particle random phase approximation: Davidson algorithm and benchmark studies,” *J. Chem. Phys.* **141**, 124104 (2014).
- ⁸⁰D. Zhang, N. Q. Su, and W. Yang, “Accurate Quasiparticle Spectra from the T-Matrix Self-Energy and the Particle–Particle Random Phase Approximation,” *J. Phys. Chem. Lett.* **8**, 3223–3227 (2017).
- ⁸¹J. Li, J. Yu, Z. Chen, and W. Yang, “Linear Scaling Calculations of Excitation Energies with Active-Space Particle–Particle Random-Phase Approximation,” *J. Phys. Chem. A* **127**, 7811–7822 (2023).
- ⁸²J. Li, Z. Chen, and W. Yang, “Renormalized Singles Green’s Function in the T-Matrix Approximation for Accurate Quasiparticle Energy Calculation,” *J. Phys. Chem. Lett.* **12**, 6203–6210 (2021).
- ⁸³R. Orlando, P. Romaniello, and P.-F. Loos, “The three channels of many-body perturbation theory: GW, particle–particle, and electron–hole T-matrix self-energies,” *J. Chem. Phys.* **159**, 184113 (2023).

- ⁸⁴A. Marie, P. Romaniello, and P.-F. Loos, “Anomalous propagators and the particle-particle channel: Hedin’s equations,” *Phys. Rev. B* **110**, 115155 (2024).
- ⁸⁵C. Sutton, Y. Yang, D. Zhang, and W. Yang, “Single, double electronic excitations and exciton effective conjugation lengths in π -conjugated systems,” *The journal of physical chemistry letters* **9**, 4029–4036 (2018).
- ⁸⁶P.-F. Loos, M. Boggio-Pasqua, A. Scemama, M. Caffarel, and D. Jacquemin, “Reference Energies for Double Excitations,” *J. Chem. Theory Comput.* **15**, 1939–1956 (2019).
- ⁸⁷W. Yang and P. W. Ayers, “Foundation for the Δ SCF approach in density functional theory,” *arXiv preprint arXiv:2403.04604* (2024).
- ⁸⁸M. N. Tahir and X. Ren, “Comparing particle-particle and particle-hole channels of the random phase approximation,” *Phys. Rev. B* **99**, 195149 (2019).
- ⁸⁹R. A. Kendall, T. H. Dunning, and R. J. Harrison, “Electron affinities of the first-row atoms revisited. systematic basis sets and wave functions,” *J. Chem. Phys.* **96**, 6796–6806 (1992).
- ⁹⁰D. E. Woon and T. H. Dunning Jr, “Gaussian basis sets for use in correlated molecular calculations. iii. the atoms aluminum through argon,” *J. Chem. Phys.* **98**, 1358–1371 (1993).
- ⁹¹Q. Sun, T. C. Berkelbach, N. S. Blunt, G. H. Booth, S. Guo, Z. Li, J. Liu, J. D. McClain, E. R. Sayfutyarova, S. Sharma, S. Wouters, and G. K.-L. Chan, “PySCF: The Python-based simulations of chemistry framework,” *WIREs Comput. Mol. Sci.* **8**, e1340 (2018).
- ⁹²Q. Sun, X. Zhang, S. Banerjee, P. Bao, M. Barbry, N. S. Blunt, N. A. Bogdanov, G. H. Booth, J. Chen, Z.-H. Cui, J. J. Eriksen, Y. Gao, S. Guo, J. Hermann, M. R. Hermes, K. Koh, P. Koval, S. Lehtola, Z. Li, J. Liu, N. Mardirossian, J. D. McClain, M. Motta, B. Mussard, H. Q. Pham, A. Pulkin, W. Purwanto, P. J. Robinson, E. Ronca, E. R. Sayfutyarova, M. Scheurer, H. F. Schurkus, J. E. T. Smith, C. Sun, S.-N. Sun, S. Upadhyay, L. K. Wagner, X. Wang, A. White, J. D. Whitfield, M. J. Williamson, S. Wouters, J. Yang, J. M. Yu, T. Zhu, T. C. Berkelbach, S. Sharma, A. Y. Sokolov, and G. K.-L. Chan, “Recent developments in the PySCF program package,” *J. Chem. Phys.* **153**, 024109 (2020).
- ⁹³T. H. Dunning, “Gaussian basis sets for use in correlated molecular calculations. I. The atoms boron through neon and hydrogen,” *J. Chem. Phys.* **90**, 1007–1023 (1989).

- ⁹⁴F. Weigend, A. Köhn, and C. Hättig, “Efficient use of the correlation consistent basis sets in resolution of the identity MP2 calculations,” *J. Chem. Phys.* **116**, 3175–3183 (2002).
- ⁹⁵A. T. Gilbert, N. A. Besley, and P. M. Gill, “Self-consistent field calculations of excited states using the maximum overlap method (mom),” *J. Phys. Chem. A* **112**, 13164–13171 (2008).
- ⁹⁶G. Davies, M. F. Hamer, and W. C. Price, “Optical studies of the 1.945 eV vibronic band in diamond,” *Proc. R. Soc. Lond. Math. Phys. Sci.* **348**, 285–298 (1997).
- ⁹⁷S. Halder, A. Mitra, M. R. Hermes, and L. Gagliardi, “Local Excitations of a Charged Nitrogen Vacancy in Diamond with Multireference Density Matrix Embedding Theory,” *J. Phys. Chem. Lett.* **14**, 4273–4280 (2023).
- ⁹⁸M. Lannoo and A. M. Stoneham, “The optical absorption of the neutral vacancy in diamond,” *J. Phys. Chem. Solids* **29**, 1987–2000 (1968).
- ⁹⁹Y. Jin, V. W.-z. Yu, M. Govoni, A. C. Xu, and G. Galli, “Excited State Properties of Point Defects in Semiconductors and Insulators Investigated with Time-Dependent Density Functional Theory,” *J. Chem. Theory Comput.* **19**, 8689–8705 (2023).
- ¹⁰⁰S. Verma, A. Mitra, Y. Jin, S. Halder, C. Vorwerk, M. R. Hermes, G. Galli, and L. Gagliardi, “Optical Properties of Neutral F Centers in Bulk MgO with Density Matrix Embedding,” *J. Phys. Chem. Lett.* **14**, 7703–7710 (2023).
- ¹⁰¹Y. Jin, M. Govoni, and G. Galli, “Vibrationally resolved optical excitations of the nitrogen-vacancy center in diamond,” *npj Comput. Mater.* **8**, 1–9 (2022).